Digital Signal Processing 83 (2018) 261–270

Contents lists available at ScienceDirect

Digital Signal Processing

www.elsevier.com/locate/dsp

An efficient method for angular parameter estimation of incoherently distributed sources via beamspace shift invariance

Zhi Zheng [a,*], Jian Lu [a], Wen-Qin Wang [a], Haifen Yang [a], Shunsheng Zhang [b]

[a] School of Information and Communication Engineering, University of Electronic Science and Technology of China, Chengdu 611731, China
[b] Research Institute Electronic Science and Technology, University of Electronic Science and Technology of China, Chengdu 611731, China

ARTICLE INFO

Article history:
Available online 20 September 2018

Keywords:
Direction-of-arrival (DOA)
Angular spread
Incoherently distributed (ID) sources
Uniform linear array (ULA)
Beamspace shift invariance

ABSTRACT

In this paper, we propose a beamspace-based method for nominal direction-of-arrival (DOA) and angular spread estimation of incoherently distributed (ID) sources using a uniform linear array (ULA). Firstly, with generalized array manifold of the ULA, we obtain the beamspace array manifold by performing beamspace transformation on the received vector of two overlapping subarrays, and further derive the beamspace shift invariance structure via designing appropriate beamforming matrix. Next, the total least squares approach is used to estimate the nominal DOAs of ID sources. Finally, with the DOA estimates, the corresponding angular spreads are obtained by means of the central moments of the angular distribution. The proposed method does not involve any spectral search and reduces the dimension of matrix operations, thus it is obviously more efficient than the traditional algorithms. Simulation results indicate that our proposed algorithm is comparable to the existing algorithms when the number of sensors is large.

1. Introduction

Source localization, which is referred to as the estimation of direction-of-arrival (DOA), is an important topic in array signal processing and has attracted considerable attention in the past decades [1]. Therefore, various high-resolution methods like MUSIC [2] and ESPRIT [3] were developed to perform DOA estimation. Most of them are based on point source model, that is, the energy of each source is assumed to be concentrated at discrete direction. But in applications such as radar, sonar, mobile communications, the angular spread effect cannot be neglected due to multipath propagation [4]. Therefore, a "scattered" or "distributed" source model is more appropriate [5,6], where the received signal is characterized by two angular parameters, i.e., the nominal DOA and the angular spread. Depending on the correlation among different rays, the distributed sources can be categorized into coherently distributed (CD) and incoherently distributed (ID) sources [7]. A source is called CD sources if the signal components arriving from different directions are delayed and scaled replicas of the same signal, whereas in the ID case, all signals coming from different directions are assumed to be uncorrelated.

In the past decades, the parameter estimation of CD sources has been well studied via extending the classical methods for point sources [7–18]. However in case of ID sources, the parameter estimation problem becomes rather complicated since the dimension of the signal or noise subspace cannot be determined. Thus, most classical methods based on point source assumption are not easily generalized to this situation. To cope with ID sources, various special approaches have also been developed on the basis of maximum likelihood (ML), pseudo-signal subspace, generalized Capon (GC) and others.

Among the existing estimators for ID sources, the ML estimator [19] can provide optimal performance, where the likelihood function is jointly maximized for all parameters of the Gaussian model. The ML estimator has heavy computational burden because it involves a multidimensional search over a nonlinear likelihood function. While the approximate ML estimators of [20,21] exhibits suboptimal performance with lower computational load. By using a simplified signal model, another approximate ML estimator was proposed in [22]. It reduces the search dimension but is limited to a single-source scenario. These approximate ML estimators are still computationally intensive.

Subspace-based approaches are another type of popular techniques. The modifications of the classical MUSIC algorithm have given rise to the distributed source parameter estimator (DSPE) [7] and dispersed signal parameter estimator (DISPARE) [23]. But both of them can not provide consistent estimates. To overcome this

* Corresponding author.
E-mail addresses: zz@uestc.edu.cn (Z. Zheng), 201621010410@std.uestc.edu.cn (J. Lu), wqwang@uestc.edu.cn (W.-Q. Wang), yanghf@uestc.edu.cn (H. Yang), zhangss_bit@163.com (S. Zhang).

https://doi.org/10.1016/j.dsp.2018.09.003
1051-2004/

drawback, a class of weighted subspace fitting algorithms in the case of full-rank data model has been developed to provide consistent parameter estimates [24,25]. Moreover, an efficient subspace-based (ESB) estimator without eigen-decomposition was proposed in [26]. The main difficulty of these subspace-based approaches is the choice of the effective dimension of the pseudo-signal subspace, since the optimal choice depends on the unknown parameters. To tackle this issue, the GC estimator [27] was presented by generalizing the Capon method [28]. However, it assumes that the multiple sources must have identical and known angular distribution. To overcome the shortcomings of [27], a robust GC algorithm was proposed in [29]. Similar to the ML estimator, these algorithms have high computational complexity due to multidimensional search.

To reduce the computational cost, some ID sources estimators based on covariance matching [30], two-ray model and ESPRIT [3] have been proposed. For instance, the COMET-EXIP method [31] replaces the multidimensional search via two successive one-dimensional (1-D) searches. However, this algorithm suffers from ambiguity problem that limits its application in practice. This ambiguity problem was later successfully solved in [32]. Moreover, [31] and [32] can only handle a single source. In [33], a search-free covariance fitting approach is presented, where the nominal DOAs and angular spreads can be obtained from the central and noncentral moments of the angular power densities. This approach can be used for widely separated multisource scenarios with different angular distributions. However, this method requires the preliminary estimates of nominal DOAs. In [34], the authors suggested a low-complexity estimator using a two-ray approximate model for distributed sources, where each source is considered as a rank two component to the array covariance matrix. The main disadvantage of this method is that it is restricted to the single source case. In [9], an ESPRIT-based method was proposed, which derives the generalized array manifold (GAM) to obtain the closed-form solutions of nominal DOAs and angular spreads. By employing the generalized ESPRIT [35], the authors of [36] have devised the generalized ESPRIT method for ID sources. Compared with the ESPRIT-based method [9], [36] can achieve better performance and deal with more sources. [9] and [36] are restricted to the array geometry with two identical and closely-deployed uniform linear arrays (ULAs) to obtain an approximate shift invariance structure, implying their limited applicability.

Beamspace transformation is one way of reducing computational complexity and sometimes improving the estimation accuracy [37–40]. In this paper, we present a beamspace-based approach for estimating the angular parameters of ID sources. First of all, with generalized array manifold of the ULA, we obtain the beamspace array manifold by performing beamspace transformation on the observed vectors of the overlapping subarrays, and establish the generalized shift invariance structure in beamspace by choosing appropriate beamforming matrix. Then, the total least squares (TLS) method is adopted to estimate the nominal DOAs of ID sources. With the DOA estimates, the angular spread estimates are finally derived from the central moments of the angular distribution. Our approach does not require any spectral search and reduces the dimension of matrix operations, thus it is computationally more attractive than the existing techniques. Simulation results verify the effectiveness of the proposed algorithm.

The paper is organized as follows. In Section 2, we present the array signal model of ID sources and some necessary assumptions. In Section 3, an efficient beamspace-based approach for localization of ID sources is described in detail. Computer simulation results are provided in Section 4, and conclusions are drawn in Section 5.

Notations The superscripts $*$, T, H, $\dagger$ and $'$ denote the conjugate, transpose, conjugate transpose, pseudo-inverse and first-order derivative, respectively. $E\{\cdot\}$ represents the statistical expectation. $\mathbf{I}_P$ stands for the $P \times P$ identity matrix, and $\mathbf{0}_{(M-1)\times 1}$ is the $(M-1)\times 1$ vector of zeros. $[\cdot]_{j,k}$ denotes the (j,k)th entry of a matrix. diag$[\cdot]$ denotes a diagonal matrix and the values in the brackets constitute its diagonal elements. $\delta(\cdot)$ is the Kronecker delta function.

2. Signal model and basic assumptions

Assume that the signals from K narrowband ID sources impinge on a ULA of M sensors. The received signal at the array can be expressed as

$$\mathbf{x}(t) = \sum_{k=1}^{K} s_k(t) \sum_{l=1}^{L_k} \gamma_{k,l}\mathbf{a}(\theta_{k,l}(t)) + \mathbf{n}(t) \tag{1}$$

where $t = 1, 2, \ldots, N$ is the sampling time, and N is the number of snapshots; $s_k(t)$ is the complex-valued signal transmitted by the kth source; L_k is the number of rays inside the kth source and $\gamma_{k,l}(t)$ is the complex-valued gain of the lth ray from the kth source; $\theta_{k,l}(t) \in (-\pi/2, \pi/2)$ is the DOA of the lth ray from the kth source; $\mathbf{n}(t) \in \mathbb{C}^{M\times 1}$ is the complex-valued additive noise vector, whose elements are spatially and temporally zero-mean white Gaussian processes with variance σ_n^2. The array manifold, $\mathbf{a}(\theta_{k,l}(t)) \in \mathbb{C}^{M\times 1}$ is the response of the array corresponding to the DOA $\theta_{k,l}(t)$, which is given by

$$\mathbf{a}(\theta_{k,l}(t)) = \left[1, e^{j\Delta \sin(\theta_{k,l}(t))}, \ldots, e^{j(M-1)\Delta \sin(\theta_{k,l}(t))}\right] \tag{2}$$

where $\Delta = 2\pi d/\lambda$, d is the distance between two adjacent sensors, and λ is the wavelength of the impinging signal.

We may represent $\theta_{k,l}(t)$ as

$$\theta_{k,l}(t) = \theta_k + \tilde{\theta}_{k,l}(t) \tag{3}$$

where θ_k is the nominal DOA of the kth source, i.e., the mean of $\theta_{k,l}(t)$; $\tilde{\theta}_{k,l}(t)$ is the corresponding random angular deviation with zero mean and standard deviation σ_k, which is referred to as the angular spread.

Throughout this paper, the following assumptions are required to hold:

(i) The angular deviation, $\tilde{\theta}_{k,l}(t)$ is temporally independent and identically distributed (i.i.d.) random variables with covariances:

$$E\{\tilde{\theta}_{k,l}(t)\tilde{\theta}_{\tilde{k},\tilde{l}}(\tilde{t})\} = \sigma_k^2\delta(k-\tilde{k})\delta(l-\tilde{l})\delta(t-\tilde{t}) \tag{4}$$

(ii) The ray gains $\gamma_{k,l}$, $k = 1, 2, \ldots, K$, $l = 1, 2, \ldots, L_k$, are temporally white and are independent from ray to ray with zero mean and covariance:

$$E\{\gamma_{k,l}(t)\gamma^*_{\tilde{k},\tilde{l}}(\tilde{t})\} = \frac{\sigma^2_{\gamma_k}}{L_k}\delta(k-\tilde{k})\delta(l-\tilde{l})\delta(t-\tilde{t}) \tag{5}$$

where $\sigma^2_{\gamma_k}$ is the ray gain variance from the kth source.

(iii) The source signals $s_k(t)$, $k = 1, 2, \ldots, K$, $t = 1, 2, \ldots, N$, are temporally i.i.d. zero-mean random variables with constant amplitudes and covariance:

$$E\{s_k(t)s^H_{\tilde{k}}(\tilde{t})\} = \sigma^2_{s_k}\delta(k-\tilde{k})\delta(t-\tilde{t}) \tag{6}$$

where $\sigma^2_{s_k} = E\{|s_k(t)|^2\}$ is the signal power of the kth source.

(iv) The source signals, angular deviations, ray gains and noise are mutually uncorrelated.

(v) The number of sources K, is known *a priori* and the number of sensors M is larger than K.

(vi) Like most previous works [5,9,19,23,26,31–33,36], the angular spreads $\{\sigma_k\}_{k=1}^K$ are assumed small.

(vii) The numbers of impinging rays $\{L_k\}_{k=1}^K$ are large.

3. Proposed method

3.1. Beamspace signal subspace

Under small angular spread, using the first-order Taylor series expansion around the nominal DOA θ_k, $\mathbf{a}(\theta_{k,l}(t))$ can be approximately written as

$$\begin{aligned}\mathbf{a}(\theta_{k,l}(t)) &= \mathbf{a}(\theta_k + \tilde{\theta}_{k,l}(t)) \\ &\approx \mathbf{a}(\theta_k) + \mathbf{a}'(\theta_k)\tilde{\theta}_{k,l}(t)\end{aligned} \tag{7}$$

where the second and higher-order terms of the Taylor series have been omitted.

Substituting (7) into (1) yields

$$\mathbf{x}(t) \approx \sum_{k=1}^{K} \left(\mathbf{a}(\theta_k)v_{k,0}(t) + \mathbf{a}'(\theta_k)v_{k,1}(t)\right) + \mathbf{n}(t) \tag{8}$$

where

$$v_{k,0}(t) = s_k(t)\sum_{l=1}^{L_k}\gamma_{k,l}(t), \tag{9}$$

$$v_{k,1}(t) = s_k(t)\sum_{l=1}^{L_k}\gamma_{k,l}(t)\tilde{\theta}_{k,l}(t). \tag{10}$$

In matrix form, (8) becomes:

$$\mathbf{x}(t) \approx \mathbf{A}\mathbf{v}(t) + \mathbf{n}(t) \tag{11}$$

where

$$\mathbf{A} = [\mathbf{a}(\theta_1), \ldots, \mathbf{a}(\theta_K), \mathbf{a}'(\theta_1), \ldots, \mathbf{a}'(\theta_K)] \tag{12}$$

is the generalized manifold matrix of the ULA, and

$$\mathbf{v}(t) = [v_{1,0}(t), \ldots, v_{K,0}(t), v_{1,1}(t), \ldots, v_{K,1}(t)]^T. \tag{13}$$

The dimension of $\mathbf{x}(t)$ can be reduced by the so-called beamspace transformation as:

$$\mathbf{y}(t) = \mathbf{W}^H\mathbf{x}(t) = \mathbf{B}\mathbf{v}(t) + \mathbf{W}^H\mathbf{n}(t) \tag{14}$$

where $\mathbf{y}(t)$ is the $P \times 1$ beamspace observed vector (P is referred to as the number of beams or beamspace dimension), $\mathbf{W}$ is the $M \times P$ beamspace transformation matrix satisfying $\mathbf{W}^H\mathbf{W} = \mathbf{I}_P$, and $\mathbf{B} = \mathbf{W}^H\mathbf{A}$ is the beamspace manifold matrix.

The covariance matrix of $\mathbf{y}(t)$ is:

$$\begin{aligned}\mathbf{R}_y &= E\{\mathbf{y}(t)\mathbf{y}^H(t)\} \\ &= E\{\mathbf{W}^H\mathbf{x}(t)\mathbf{x}^H(t)\mathbf{W}\} \\ &= \mathbf{B}\mathbf{\Lambda}_v\mathbf{B}^H + \sigma_n^2\mathbf{I}_P\end{aligned} \tag{15}$$

where

$$\mathbf{\Lambda}_v = E\{\mathbf{v}(t)\mathbf{v}^H(t)\}. \tag{16}$$

According to the properties of $\tilde{\theta}_{k,l}$, $\gamma_{k,l}$ and $s_k(t)$ given in (4)–(6) and the assumption that the source signals, angular deviations and ray gains are mutually uncorrelated, we obtain

$$E\{v_{k,0}(t)v_{k,0}^*(t)\} = \sigma_{s_k}^2\sigma_{\gamma_k}^2, \tag{17}$$

$$E\{v_{k,1}(t)v_{k,1}^*(t)\} = \sigma_{s_k}^2\sigma_{\gamma_k}^2\sigma_k^2, \tag{18}$$

$$E\{v_{k,l}(t)v_{\tilde{k},\tilde{l}}^*(t)\} = 0, \ \forall k \neq \tilde{k}, \ \text{or} \ l \neq \tilde{l}. \tag{19}$$

Hence, we conclude that $\mathbf{\Lambda}_v$ is a diagonal matrix with $[\mathbf{\Lambda}_v]_{k,k} = \sigma_{s_k}^2\sigma_{\gamma_k}^2$, $[\mathbf{\Lambda}_v]_{K+k,K+k} = \sigma_{s_k}^2\sigma_{\gamma_k}^2\sigma_k^2$, $k = 1, 2, \ldots, K$. From the diagonal elements of $\mathbf{\Lambda}_v$, the angular spread σ_k can be found easily.

Performing eigenvalue decomposition (EVD) of $\mathbf{R}_y$ yields

$$\mathbf{R}_y = \mathbf{U}_s\mathbf{\Sigma}_s\mathbf{U}_s^H + \mathbf{U}_n\mathbf{\Sigma}_n\mathbf{U}_n^H \tag{20}$$

where $\mathbf{\Sigma}_s \in \mathbb{C}^{2K\times 2K}$ and $\mathbf{\Sigma}_n \in \mathbb{C}^{(P-2K)\times(P-2K)}$ are the diagonal matrices containing the $2K$ largest and $(P-2K)$ smallest eigenvalues of $\mathbf{R}_y$, respectively; $\mathbf{U}_s \in \mathbb{C}^{P\times 2K}$ and $\mathbf{U}_n \in \mathbb{C}^{P\times(P-2K)}$ are composed of the eigenvectors of $\mathbf{R}_y$ corresponding to the $2K$ largest and $(P-2K)$ smallest eigenvalues, respectively, which are referred to as the beamspace signal and noise subspaces, respectively.

Based on the subspace theory, $\mathbf{U}_s$ spans the column space of $\mathbf{B}$. This means that there is a $2K \times 2K$ nonsingular matrix $\mathbf{T}$ such that

$$\mathbf{B} = \mathbf{U}_s\mathbf{T}. \tag{21}$$

Equation (21) shows the linear relationship between beamspace array manifold matrix $\mathbf{B}$ and beamspace signal subspace $\mathbf{U}_s$, which can be used to estimate the nominal DOAs of ID sources.

3.2. Nominal DOA and angular spread estimation

As is well known, the shift invariance structure between array manifolds can be utilized to achieve closed-form DOA estimates [3]. However, the shift invariance structure may be destroyed after beamspace transformation [37]. To restore the lost shift invariance property, the beamforming matrix $\mathbf{W}$ should have the same shift invariance structure. In the case of ID sources, to find the such $\mathbf{W}$, we have the theorem:

Theorem 1. *Let $\mathbf{W} \in \mathbb{C}^{M\times P}$ $(P < M)$ be a unitary matrix, i.e., $\mathbf{W}^H\mathbf{W} = \mathbf{I}_P$. Assume that the first $(M-1)$ rows and the last $(M-1)$ rows of $\mathbf{W}$ share the same column span, i.e.*

$$\mathbf{J}_1\mathbf{W} = \mathbf{J}_2\mathbf{W}\mathbf{F} \tag{22}$$

where $\mathbf{J}_1 = [\mathbf{I}_{M-1}, \mathbf{0}_{(M-1)\times 1}]$ and $\mathbf{J}_2 = [\mathbf{0}_{(M-1)\times 1}, \mathbf{I}_{M-1}]$ are selection matrices, and $\mathbf{F}$ is a $P \times P$ nonsingular matrix. Let $\mathbf{W}^H = [\mathbf{w}_1, \mathbf{w}_2, \ldots, \mathbf{w}_M]$. If there is a $P \times P$ matrix $\mathbf{Q}$ such that $\mathbf{Q}\mathbf{w}_M = \mathbf{0}_{P\times 1}$ and $\mathbf{Q}\mathbf{F}^H\mathbf{w}_1 = \mathbf{0}_{P\times 1}$, then

$$\mathbf{Q}\mathbf{B} = \mathbf{Q}\mathbf{F}^H\mathbf{B}\mathbf{\Phi} \tag{23}$$

where

$$\mathbf{\Phi} = \begin{bmatrix} \mathbf{\Lambda}_{1,1} & \mathbf{\Lambda}_{1,2} \\ \mathbf{0}_{K\times K} & \mathbf{\Lambda}_{1,1} \end{bmatrix} \tag{24}$$

with

$$\mathbf{\Lambda}_{1,1} = \mathrm{diag}[h(\theta_1), h(\theta_2), \ldots, h(\theta_K)], \tag{25}$$

$$\mathbf{\Lambda}_{1,2} = \mathrm{diag}[h'(\theta_1), h'(\theta_2), \ldots, h'(\theta_K)], \tag{26}$$

$$h(\theta_k) = e^{j\Delta\sin\theta_k}, \ \ k = 1, 2, \ldots, K. \tag{27}$$

Proof. Please refer to Appendix A. □

Theorem 1 provides a way of restoring the shift invariance property in beamspace. If $\mathbf{W} = [\mathbf{t}_1, \mathbf{t}_2, \ldots, \mathbf{t}_P]$ is the collection of standard Fourier basis vectors, i.e.,

$$\mathbf{t}_p = \frac{1}{\sqrt{M}}\left[1, e^{j2\pi p/M}, \ldots, e^{j2\pi p(M-1)/M}\right]^T, \tag{28}$$

$p = 1, 2, \ldots, P$, $\mathbf{F}$ and $\mathbf{Q}$ are easy to be constructed as

$$\mathbf{F} = \mathrm{diag}\left[e^{-j2\pi/M}, \ldots, e^{-j2\pi P/M}\right], \tag{29}$$

$$\mathbf{Q} = \mathbf{J}_Q \boldsymbol{\Gamma} \tag{30}$$

where

$$\mathbf{J}_Q = \begin{bmatrix} 1 & -1 & \ldots & 0 & 0 \\ 0 & 1 & -1 & \ldots & 0 \\ \vdots & \vdots & \ddots & \vdots & \vdots \\ 0 & 0 & \ldots & 1 & -1 \\ 0 & 0 & \ldots & 0 & 0 \end{bmatrix} \in \mathbb{C}^{P\times P},$$

$$\boldsymbol{\Gamma} = \mathrm{diag}\left[e^{j2\pi(M-1)/M}, \ldots, e^{j2\pi P(M-1)/M}\right]. \tag{31}$$

Equation (23) shows the shift invariance relationship between the array manifolds. But it cannot be used directly to estimate the nominal DOAs because $\mathbf{B}$ is also related to the nominal DOAs. According to (21), we can also derive the shift invariance relationship between beamspace signal subspaces.

Substituting (21) into (23) yields

$$\mathbf{Q}\mathbf{U}_s\mathbf{T} = \mathbf{Q}\mathbf{F}^H\mathbf{U}_s\mathbf{T}\boldsymbol{\Phi}. \tag{32}$$

Further, we have

$$\mathbf{Q}\mathbf{U}_s = \mathbf{Q}\mathbf{F}^H\mathbf{U}_s\mathbf{T}\boldsymbol{\Phi}\mathbf{T}^{-1}. \tag{33}$$

Using the definition $\boldsymbol{\Psi} = \mathbf{T}\boldsymbol{\Phi}\mathbf{T}^{-1}$, (33) can be rewritten as

$$\mathbf{Q}\mathbf{U}_s = \mathbf{Q}\mathbf{F}^H\mathbf{U}_s\boldsymbol{\Psi}. \tag{34}$$

Equation (34) can be solved by the total least squares (TLS) criterion [3] to find $\boldsymbol{\Psi}$ whose eigenvalues are related to the nominal DOAs of sources. The solving procedure is given as follows.

Define $\mathbf{G}$ as

$$\mathbf{G} = [\mathbf{Q}\mathbf{F}^H\mathbf{U}_s, \mathbf{Q}\mathbf{U}_s]^H[\mathbf{Q}\mathbf{F}^H\mathbf{U}_s, \mathbf{Q}\mathbf{U}_s]. \tag{35}$$

Performing EVD on $\mathbf{G}$ yields:

$$\mathbf{F} = \mathbf{E}_x\boldsymbol{\Lambda}_x\mathbf{E}_x^H \tag{36}$$

where $\boldsymbol{\Lambda}_x \in \mathbb{C}^{4K\times 4K}$ is the diagonal matrix containing the $4K$ eigenvalues of $\mathbf{G}$, while $\mathbf{E}_x \in \mathbb{C}^{4K\times 4K}$ is composed of the eigenvectors of $\mathbf{G}$ corresponding to the $4K$ eigenvalues.

Then $\mathbf{E}_x$ is partitioned as

$$\mathbf{E}_x = \begin{bmatrix} \mathbf{E}_{x11} & \mathbf{E}_{x12} \\ \mathbf{E}_{x21} & \mathbf{E}_{x22} \end{bmatrix}$$

where $\mathbf{E}_{xab} \in \mathbb{C}^{2K\times 2K}$, $a, b = 1, 2$.

Finally, the solution of $\boldsymbol{\Psi}$ is given by

$$\hat{\boldsymbol{\Psi}} = -\mathbf{E}_{x12}\mathbf{E}_{x22}^{-1}. \tag{37}$$

Assume that $\xi_{1,q}$, $(q = 1, 2, \ldots, 2K)$ is the qth eigenvalue of $\hat{\boldsymbol{\Psi}}$, i.e., the estimates of the diagonal elements of $\boldsymbol{\Phi}$. Let $\xi_{1,2(k-1)+r}$ be the estimate of $[\boldsymbol{\Phi}]_{k+(r-1)K,k+(r-1)K}$, $r = 1, 2$. According to (27), we have

$$\xi_{1,2(k-1)+r} \approx e^{j\Delta\sin\theta_k} \tag{38}$$

where $k = 1, 2, \ldots, K$, and $r = 1, 2$.

Then the nominal DOA of the k source is estimated as

$$\hat{\theta}_k = \frac{1}{2}\sum_{r=1}^{2}\sin^{-1}\left(\frac{\ln(\xi_{1,2(k-1)+r})}{j\Delta}\right) \tag{39}$$

Algorithm 1 Estimation of nominal DOAs and angular spreads.

1: Apply beamspace transformation (14) on element-space observed vector $\mathbf{x}(t)$ to obtain beamspace observed vector $\mathbf{y}(t)$.
2: Calculate the beamspace sample covariance matrix $\hat{\mathbf{R}}_y = (1/N)\sum_{t=1}^{N}\mathbf{y}(t)\mathbf{y}^H(t)$, and perform EVD on $\hat{\mathbf{R}}_y$ to obtain the beamspace signal subspace $\mathbf{U}_s$.
3: Calculate (34) by substituting (21) into (23), and obtain $\hat{\boldsymbol{\Psi}}$ as total least squares solution to (34).
4: Estimate the nominal DOAs using (39), and find the angular spreads via (41).

Table 1
Computational complexities of various algorithms.

Algorithm	Complexity
Proposed	$O(PMN + P^2N + P^3)$
DISPARE	$O(M^3 + M^2N + (M^2+M)^2S_\theta S_\sigma)$
GC	$O(M^3 + M^2N + (M^2+M)^2S_\theta S_\sigma)$
ESB	$O(M^2N + (M^2+M)^2S_\theta S_\sigma)$

where $k = 1, 2, \ldots, K$. Note that according to the definition of $\boldsymbol{\Phi}$, all eigenvalues of $\boldsymbol{\Psi}$ are repeated with order 2. Hence, averaging should be used to determine the nominal DOA of each source from the eigenvalues of $\hat{\boldsymbol{\Psi}}$.

From (15), we derive the estimate of $\boldsymbol{\Lambda}_v$ as

$$\hat{\boldsymbol{\Lambda}}_v = \hat{\mathbf{B}}^\dagger(\mathbf{R}_y - \hat{\sigma}_n^2\mathbf{I}_P)(\hat{\mathbf{B}}^H)^\dagger \tag{40}$$

where $\hat{\mathbf{B}} = \mathbf{W}^H\hat{\mathbf{A}}$, $\hat{\mathbf{A}}$ denotes the estimate of $\mathbf{A}$, which is obtained by replacing the nominal DOAs in $\mathbf{A}$ with $\{\hat{\theta}_k\}_{k=1}^K$. $\hat{\sigma}_n^2$ is the estimated noise variance, which can be calculated as the average of the $P-2K$ smallest eigenvalues of $\mathbf{R}_y$.

According to the definition of $\boldsymbol{\Lambda}_v$, the estimate of σ_k is given by

$$\hat{\sigma}_k = \sqrt{\frac{[\hat{\boldsymbol{\Lambda}}_v]_{K+k,K+k}}{[\hat{\boldsymbol{\Lambda}}_v]_{k,k}}}, \quad k = 1, 2, \ldots, K. \tag{41}$$

Note that $\hat{\theta}_k$ and $\hat{\sigma}_k$ are automatically paired without any extra processing. That is to say, $\hat{\theta}_k$ and $\hat{\sigma}_k$ are corresponding to the same source.

The proposed algorithm is summarized in Algorithm 1.

3.3. Computational complexity analysis

Here, we analyze the computational complexity of the proposed algorithm in comparison with the DISPARE [23], ESB [26] and GC [27] algorithms. For the proposed algorithm, the main computations include beamspace transformation, computation and EVD of $\hat{\mathbf{R}}_y$, and the multiplications required are $O(PMN + P^2N + P^3)$. While the complexities of the DISPARE and GC algorithms are mainly dominated by the computation and EVD of the sample covariance matrix, and two-dimensional (2-D) search, the resulting multiplications are $O(M^3 + M^2N + (M^2+M)^2S_\theta S_\sigma)$, where S_θ and S_σ are respectively the search dimension in the DOA domain and angular spread domain. Although the EVD of the sample covariance matrix is avoided, the ESB method still involves 2-D search, which requires $O(M^2N + (M^2+M)^2S_\theta S_\sigma)$. Noted that $S_\theta, S_\sigma \gg 1$ and $P < M$. For the sake of clarity, the computational complexities of the compared algorithms are summarized in Table 1. It is clear that the computational complexity of the proposed algorithm is obviously lower than those of the other schemes.

4. Simulation results

In this section, we provide simulation results to illustrate the performance of the proposed algorithm in comparison with some

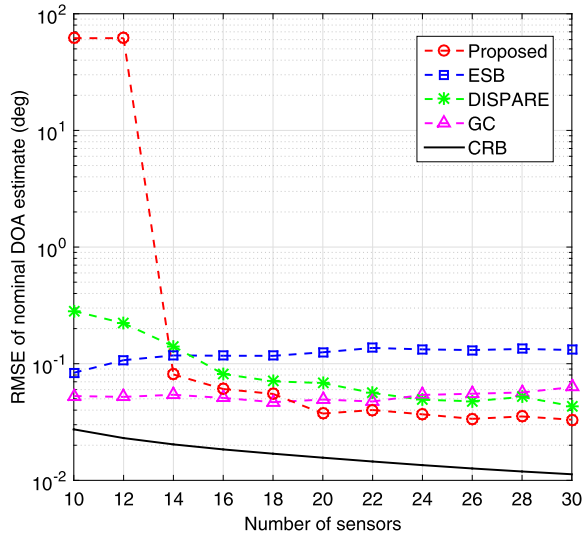

(a)

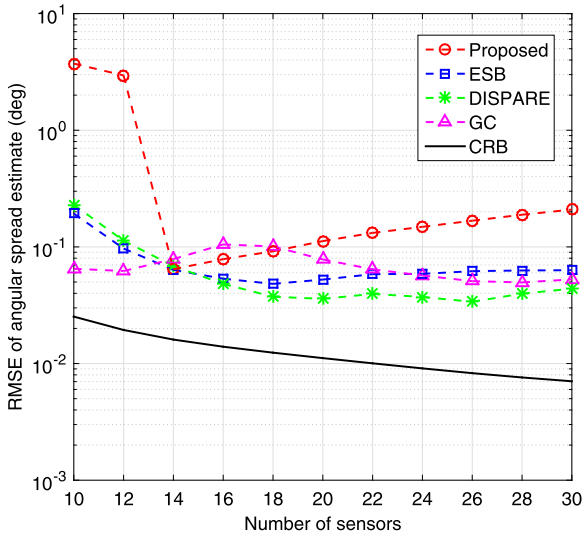

(b)

Fig. 1. RMSEs of nominal DOA and angular spread estimates versus number of sensors for two ID sources with $(\theta_1, \sigma_1) = (20°, 1°)$ and $(\theta_2, \sigma_2) = (40°, 1°)$, SNR = 20 dB, $N = 400$. (a) Nominal DOA estimation. (b) Angular spread estimation.

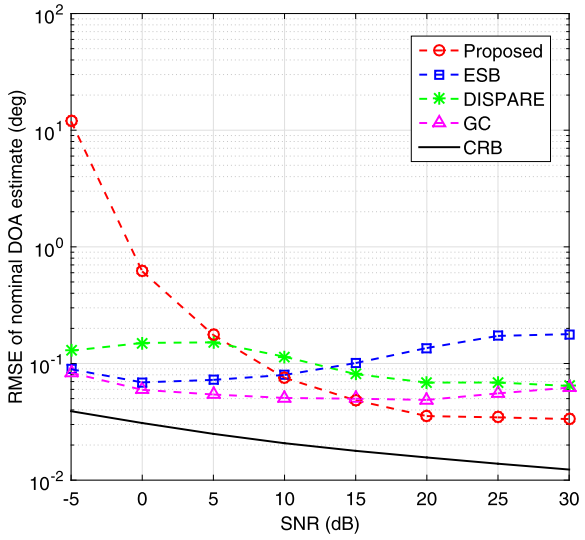

(a)

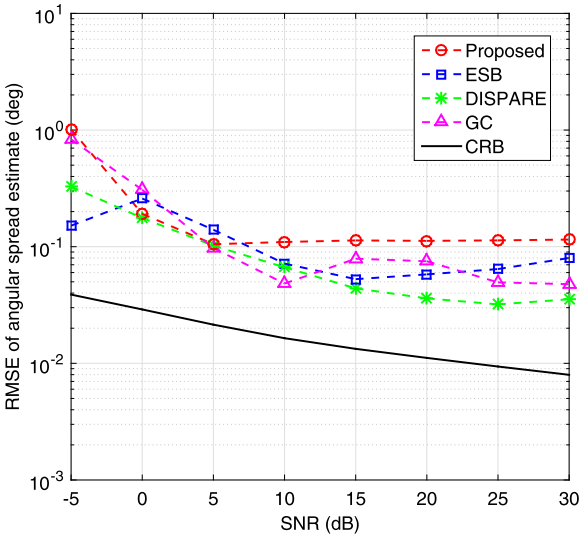

(b)

Fig. 2. RMSEs of nominal DOA and angular spread estimates versus SNR for two ID sources with $(\theta_1, \sigma_1) = (20°, 1°)$ and $(\theta_2, \sigma_2) = (40°, 1°)$, $M = 20$, $N = 400$. (a) Nominal DOA estimation. (b) Angular spread estimation.

known estimators, DISPARE [23], ESB [26], GC [27] as well as the Cramer–Rao bound (CRB) [6]. In our simulations, a ULA with M sensors separated by a half wavelength is considered. The received signal-to-noise ratio (SNR) from the kth source is defined as $10\log_{10}(\sigma_{s_k}^2/\sigma_n^2)$. Assume that all ID sources have Gaussian-shaped angular distribution, the variance of ray gain is $\{\sigma_{\gamma_k}^2\}_{k=1}^K = 1$, and the number of incoming rays is $\{L_k\}_{k=1}^K = 80$. For [23], [26] and [27], the searching interval of the nominal DOAs is 0.05°, while the searching interval of the angular spreads is 0.01°. The results are evaluated by the estimated root mean square error (RMSE) from the average results of 300 independent trials.

In the first example, we assess the performance of the proposed approach with respect to the number of sensors. For this simulation, two ID sources with angular parameters $(\theta_1, \sigma_1) = (20°, 1°)$ and $(\theta_2, \sigma_2) = (40°, 1°)$ are considered. The number of beams is set as $P = M - 2$ for the proposed method. The number of sensors varies from 10 to 30, SNR = 20 dB and the number of snapshots is $N = 400$. Figs. 1(a) and 1(b) plot respectively the RMSEs of nominal DOA and angular spread estimates versus number of sensors. We can see from Fig. 1(a) that the performances of the proposed and DISPARE methods improve gradually as the number of sensors increases, while those of the ESB and GC methods are almost insensitive to M. More specifically, when the number of sensors is more than 12, the RMSE of the proposed method will decrease rapidly, and is even smaller than that of other algorithms. As shown in Fig. 1(b), when the number of sensors exceeds 12, the proposed algorithm is comparable to other algorithms for angular spread estimation. Furthermore, the performance of the proposed algorithm slowly degrade as the number of sensors increases, while that of other algorithms remains relatively stable.

In the second example, we examine the performance of the proposed algorithm for different SNRs. The SNR varies from -5 dB to 30 dB, $M = 20$ and $P = 15$, while the other simulation parameters are the same as those in the first example. Figs. 2(a) and 2(b) display respectively the RMSEs of nominal DOA and angular spread estimates versus SNR. From Fig. 2(a), we see that when the SNR is low, the proposed algorithm suffers significant performance degradation compared with other schemes, but the RMSEs of nominal DOA estimates of the proposed algorithm decrease rapidly as the SNR increases. When the SNR exceeds 15 dB, the proposed algorithm outperforms the remaining methods. By comparison, the performances of the DISPARE, ESB and GC methods remain relatively constant across a wide range of SNR. As it can be seen from Fig. 2(b), all algorithms improve angular spread estimates as the SNR increases, but the performance of the proposed algorithm is almost unchanged when the SNR is more than 5 dB. These simulation results indicate that the SNR has the same impact on performance as the number of sensors, as shown in Fig. 1. Hence, our approach can achieve good performance even at low SNRs by employing a large number of sensors.

In the third example, we test the performance of the proposed approach in terms of the number of snapshots. The number of snapshots varies from 100 to 1000, and the SNR is fixed at 20 dB, while the other simulation parameters are the same as those in the second example. Figs. 3(a) and 3(b) depict respectively the RMSEs of nominal DOA and angular spread estimates versus number of snapshots. We observe from Fig. 3(a) that the RMSEs of nominal DOA estimates of all these approaches decrease gradually as the number of snapshots increases. On the other side, when the number of snapshots increases, the DISPARE and ESB methods achieve angular spread estimates with smaller RMSEs, while the proposed and GC methods exhibit relatively stable estimates, as compared in Fig. 3(b).

In the fourth example, we investigate the performance of the proposed algorithm when the angular spread increases. The nominal DOAs of two sources are fixed at $\theta_1 = 20^\circ$ and $\theta_2 = 40^\circ$, their angular spreads are varied from 0.1° to 1.2°, SNR $= 20$ dB, while the other simulation parameters are the same as those in the second example. The RMSEs of nominal DOA and angular spread estimates versus angular spread are respectively shown in Figs. 4(a) and 4(b). It is observed that the proposed method achieves best performance when the angular spread is in the middle of the range. When the angular spread is small, the diagonal elements of $\mathbf{\Lambda}_v$ are also small. Hence, the impact of the noise becomes more prominent and the proposed algorithm will suffer severe performance degradation. When the angular spread is large, the performance of the proposed method will also degrade because the higher-order terms of the Taylor series in (7) cannot be neglected. However, the performances of the DISPARE, ESB and GC methods steadily degrade as the angular spread increases. That is because the Taylor approximation of the array manifolds in these methods differ from that of the proposed method, the estimation performance of [23], [26] and [27] are mainly determined by the higher-order terms of the Taylor series rather than by the noise. Furthermore, the proposed algorithm achieves angular spread estimates with smaller RMSEs than other three methods when the angular spread belongs to $[0.2^\circ, 0.6^\circ]$. Thus, our algorithm has highest estimation accuracy when the angular spread is neither too small nor too large.

In the fifth example, we evaluate the performance of the proposed algorithm against the DOA separation between two ID sources. Assume that two sources have the same angular spread $\sigma_1 = \sigma_2 = 1^\circ$. One source is located at $\theta_1 = 40^\circ$, and the other is from the direction $\theta_2 = 40^\circ + \delta$, where δ varies from 2° to 20°. The SNR is equal to 20 dB, while the other simulation parameters are the same as those in the second example. The RMSEs of nominal DOA and angular spread estimates versus DOA separation are respectively plotted in Figs. 5(a) and 5(b). It can be seen from 5(a) that the proposed algorithm exhibits worse estimation performance than other methods for nominal DOAs when the DOA separation is small, but the performance of the proposed algorithm is gradually close to or even exceeds that of [23] and [26] as the DOA separation increases. It can also be seen from 5(b) that as the DOA separation increases, the RMSEs of angular spread estimates of the proposed algorithm gradually decrease, and reach a relative stable value when the DOA separation is more than 6°. Moreover, the angular spread estimates of the proposed algorithm are comparable to those of other schemes when the DOA separation is greater than 4°.

In the last example, we illustrate the effect of the number of beams on the performance of the proposed algorithm. In this

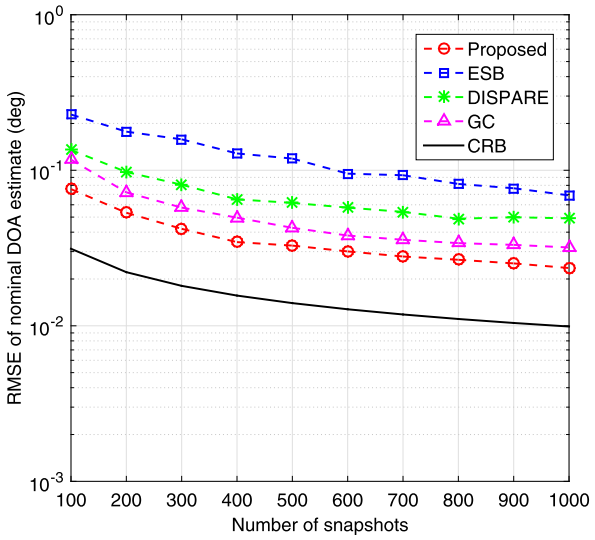

(a)

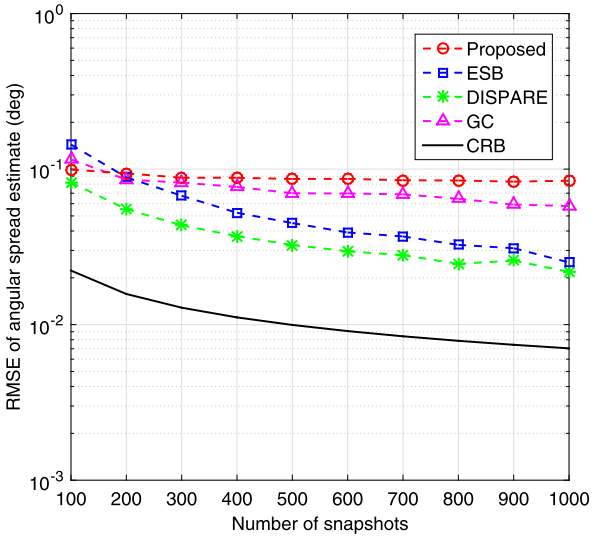

(b)

Fig. 3. RMSEs of nominal DOA and angular spread estimates versus number of snapshots for two ID sources with $(\theta_1, \sigma_1) = (20^\circ, 1^\circ)$ and $(\theta_2, \sigma_2) = (40^\circ, 1^\circ)$, $M = 20$, SNR $= 20$ dB. (a) Nominal DOA estimation. (b) Angular spread estimation.

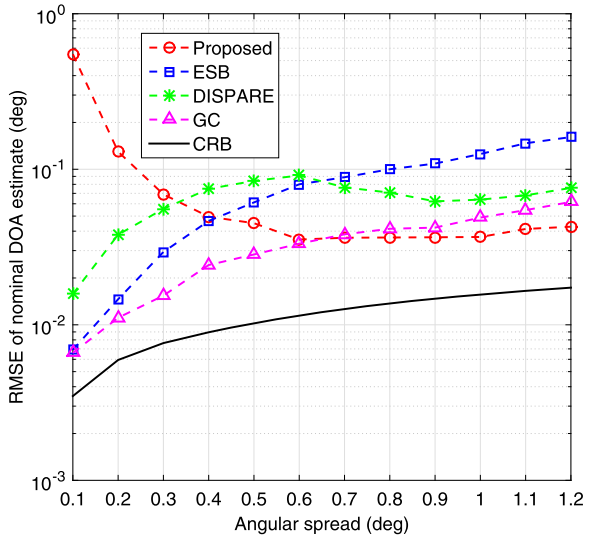

(a)

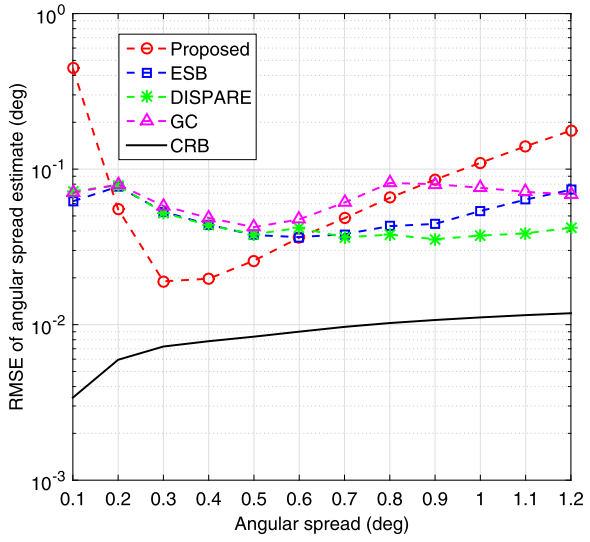

(b)

Fig. 4. RMSEs of nominal DOA and angular spread estimates versus angular spread for two ID sources with $\theta_1 = 20°$ and $\theta_2 = 40°$, $M = 20$, SNR $= 20$ dB, $N = 400$. (a) Nominal DOA estimation. (b) Angular spread estimation.

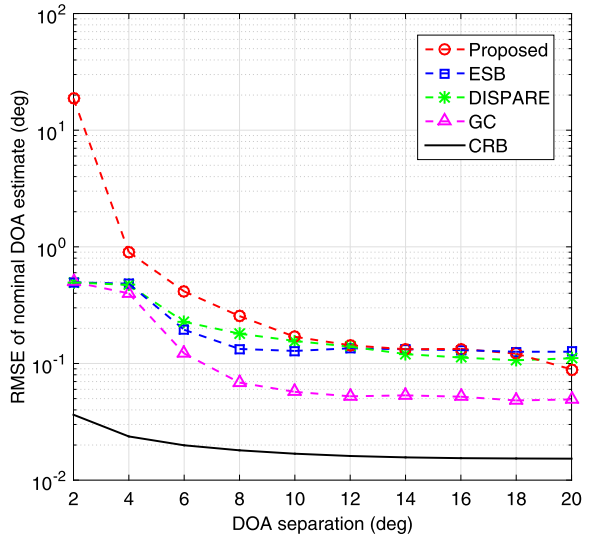

(a)

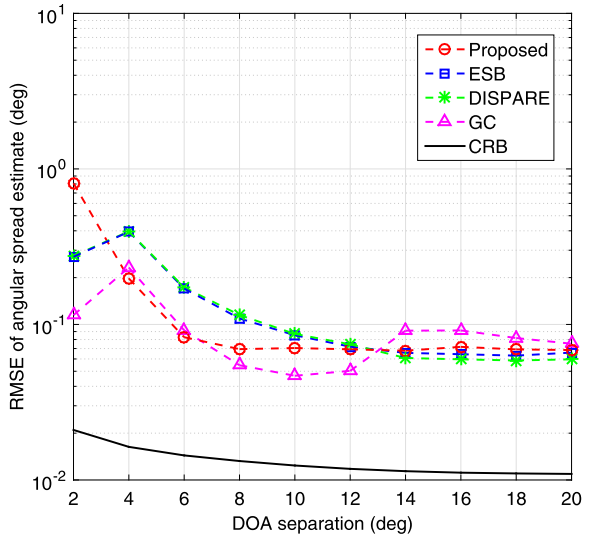

(b)

Fig. 5. RMSEs of nominal DOA and angular spread estimates versus DOA separation for two ID sources with $(\theta_1, \sigma_1) = (40°, 1°)$ and $(\theta_2, \sigma_2) = (40° + \delta, 1°)$, $M = 20$, SNR $= 20$ dB, $N = 400$. (a) Nominal DOA estimation. (b) Angular spread estimation.

example, we consider three ID sources with angular parameters $(\theta_1, \sigma_1) = (20°, 1°)$, $(\theta_2, \sigma_2) = (40°, 1°)$ and $(\theta_3, \sigma_3) = (70°, 1°)$. The number of beams is varied from 8 to 18, while the other simulation parameters are the same as those in the fifth example. The RMSEs of nominal DOA and angular spread estimates versus number of beams are respectively demonstrated in Figs. 6(a) and 6(b). As shown in these figures, when the number of beams is small, the proposed algorithm suffers severe performance degradation compared with other algorithms. When the number of beams is more than 10, the RMSEs of the proposed algorithm decrease rapidly and stay in a stable level. In contrast, the RMSEs of the DISPARE, ESB and GC methods remains unchanged in the whole range of number of beams. That is because the algorithms in [23], [26] and [27] are performed in the element space, while the proposed approach is implemented in beamspace and its subspace estimation accuracy is related to the number of beams.

5. Conclusions

In this paper, an efficient algorithm for nominal DOA and angular spread estimation of ID sources has been introduced. The proposed algorithm is developed based on the ULA and small angular spread assumption. By choosing appropriate beamforming matrix and overlapping subarrays, we obtain the generalized shift invariance structure in beamspace, from which the nominal DOA estimates are derived. With the estimated DOAs, the angular spreads can be given in closed-form solutions. Compared with the traditional schemes, the proposed algorithm avoids spectral search and reduce the dimension of matrix operations. Therefore, it has much lower computational complexity. Simulation results show that the performance of the proposed algorithm is comparable to those of the traditional algorithms when the number of sensors is large.

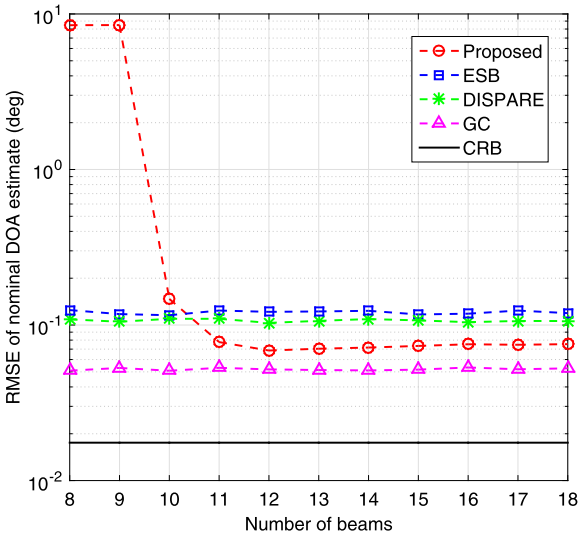

(a)

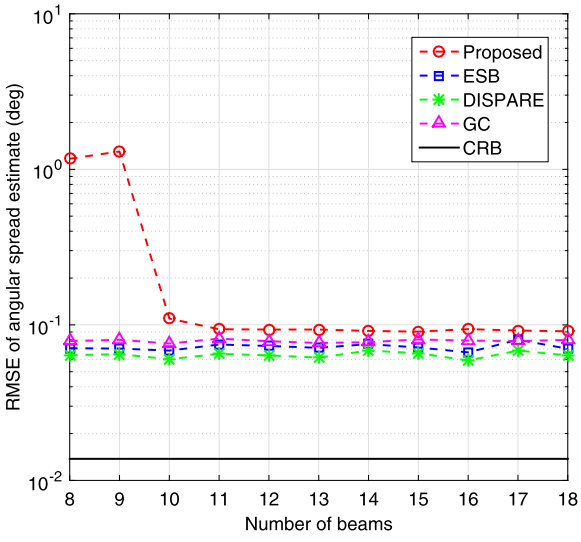

(b)

Fig. 6. RMSEs of nominal DOA and angular spread estimates versus number of beams for three ID sources with $(\theta_1, \sigma_1) = (20°, 1°)$, $(\theta_2, \sigma_2) = (40°, 1°)$ and $(\theta_3, \sigma_3) = (70°, 1°)$, $M = 20$, SNR $= 20$ dB, $N = 400$. (a) Nominal DOA estimation. (b) Angular spread estimation.

Acknowledgments

This work is supported in part by the National Natural Science Foundation of China under Grants 61301155, 61571081 and 61703076, by Sichuan Science and Technology Program under Grant 2018RZ0141, by the Key Project of Sichuan Education Department of China under Grant 18ZA0221, and by the Fundamental Research Funds for the Central Universities of China under Grants ZYGX2016J008 and 2672018ZYGX2018J003.

Appendix A. Proof of Theorem 1

Consider two maximally overlapping subarrays of the ULA, their array manifolds are expressed as

$$\mathbf{a}_1(\theta_k) = \mathbf{J}_1\mathbf{a}(\theta_k), \tag{42}$$

$$\mathbf{a}_2(\theta_k) = \mathbf{J}_2\mathbf{a}(\theta_k). \tag{43}$$

Then, we get

$$\mathbf{a}_2(\theta_k) = h(\theta_k)\mathbf{a}_1(\theta_k). \tag{44}$$

The first-order derivative of $\mathbf{a}_2(\theta_k)$ around θ_k is expressed as

$$\mathbf{a}_2'(\theta_k) = h(\theta_k)\mathbf{a}_1'(\theta_k) + h'(\theta_k)\mathbf{a}_1(\theta_k). \tag{45}$$

The generalized manifold matrix of the ith subarray is:

$$\begin{aligned}\mathbf{A}_i &= \mathbf{J}_i\mathbf{A}\\ &= [\mathbf{a}_i(\theta_1), \ldots, \mathbf{a}_i(\theta_K), \mathbf{a}_i'(\theta_1), \ldots, \mathbf{a}_i'(\theta_K)]\\ &\in \mathbb{C}^{(M-1)\times 2K}, \quad i = 1, 2.\end{aligned} \tag{46}$$

Based on (44)–(46), the manifold matrices of the overlapping subarrays are linearly related as

$$\mathbf{A}_2 = \mathbf{A}_1\mathbf{\Phi}. \tag{47}$$

Further, we can obtain

$$\mathbf{J}_1\mathbf{A} = \mathbf{J}_2\mathbf{A}\mathbf{\Phi}. \tag{48}$$

By the condition of $\mathbf{Q}$:

$$\begin{aligned}\mathbf{Q}\mathbf{W}^H &= [\mathbf{Q}\mathbf{w}_1, \mathbf{Q}\mathbf{w}_2, \ldots, \mathbf{Q}\mathbf{w}_{M-1}, \mathbf{0}_{P\times 1}]\\ &= \mathbf{Q}\mathbf{W}^H\mathbf{J}_1^H\mathbf{J}_1,\end{aligned} \tag{49}$$

$$\begin{aligned}\mathbf{Q}\mathbf{F}^H\mathbf{W}^H &= [\mathbf{0}_{P\times 1}, \mathbf{Q}\mathbf{F}^H\mathbf{w}_2, \ldots, \mathbf{Q}\mathbf{F}^H\mathbf{w}_M]\\ &= \mathbf{Q}\mathbf{F}^H\mathbf{W}^H\mathbf{J}_2^H\mathbf{J}_2.\end{aligned} \tag{50}$$

Consequently,

$$\mathbf{Q}\mathbf{B} = \mathbf{Q}\mathbf{W}^H\mathbf{A} = \mathbf{Q}\mathbf{W}^H\mathbf{J}_1^H\mathbf{J}_1\mathbf{A}. \tag{51}$$

Using (48) and the conjugate transpose of (22), viz., $\mathbf{W}^H\mathbf{J}_1^H = \mathbf{F}^H\mathbf{W}^H\mathbf{J}_2^H$, we obtain

$$\mathbf{Q}\mathbf{B} = \mathbf{Q}\overbrace{\mathbf{W}^H\mathbf{J}_1^H}\overbrace{\mathbf{J}_1\mathbf{A}} = \mathbf{Q}\overbrace{\mathbf{F}^H\mathbf{W}^H\mathbf{J}_2^H}\overbrace{\mathbf{J}_2\mathbf{A}\mathbf{\Phi}}. \tag{52}$$

From (50), we have:

$$\mathbf{Q}\mathbf{F}^H\mathbf{B} = \overbrace{\mathbf{Q}\mathbf{F}^H\mathbf{W}^H}\mathbf{A} = \overbrace{\mathbf{Q}\mathbf{F}^H\mathbf{W}^H\mathbf{J}_2^H\mathbf{J}_2}\mathbf{A}. \tag{53}$$

Comparing (52) and (53) yields:

$$\mathbf{Q}\mathbf{B} = \mathbf{Q}\mathbf{F}^H\mathbf{B}\mathbf{\Phi}. \tag{54}$$

References

[1] H. Krim, M. Viberg, Two decades of array signal processing research: the parametric approach, IEEE Signal Process. Mag. 13 (4) (Jul. 1996) 67–94.
[2] R. Schmidt, Multiple emitter location and signal parameter estimation, IEEE Trans. Antennas Propag. 34 (3) (Mar. 1986) 276–280.
[3] R. Roy, T. Kailath, ESPRIT-estimation of signal parameters via rotational invariance techniques, IEEE Trans. Acoust. Speech Signal Process. 37 (7) (Jul. 1989) 984–995.
[4] P. Zetterberg, B. Ottersten, The spectrum efficiency of a base station antenna array system for spatially selective transmission, IEEE Trans. Veh. Technol. 44 (3) (Aug. 1995) 651–660.
[5] D. Astely, B. Ottersten, The effects of local scattering on direction of arrival estimation with MUSIC, IEEE Trans. Signal Process. 47 (12) (Dec. 1999) 3220–3234.
[6] R. Raich, J. Goldberg, H. Messer, Bearing estimation for a distributed source: modeling, inherent accuracy limitations and algorithms, IEEE Trans. Signal Process. 48 (2) (Feb. 2000) 429–441.

[7] S. Valaee, B. Champagne, P. Kabal, Parametric localization of distributed sources, IEEE Trans. Signal Process. 43 (9) (Sep. 1995) 2144–2153.
[8] Y.U. Lee, J. Choi, I. Song, S.R. Lee, Distributed source modeling and direction-of-arrival estimation techniques, IEEE Trans. Signal Process. 45 (4) (Apr. 1997) 960–969.
[9] S. Shahbazpanahi, S. Valaee, M.H. Bastani, Distributed source localization using ESPRIT algorithm, IEEE Trans. Signal Process. 49 (10) (Oct. 2001) 2169–2178.
[10] J. Lee, I. Song, H. Kwon, S.R. Lee, Low-complexity estimation of 2D DOA for coherently distributed sources, Signal Process. 83 (8) (Aug. 2003) 1789–1802.
[11] M. Agrawal, P. Stoica, O. Besson, P. Åhgren, Estimation of nominal directions of arrival and angular spreads of distributed sources, Signal Process. 83 (8) (Aug. 2003) 1833–1838.
[12] X. Guo, Q. Wan, B. Wu, W. Yang, Parameters localisation of coherently distributed sources based on sparse signal representation, IET Radar Sonar Navig. 1 (4) (Aug. 2007) 261–265.
[13] A. Zoubir, Y. Wang, Efficient DSPE algorithm for estimating the angular parameters of coherently distributed sources, Signal Process. 88 (4) (Apr. 2008) 1071–1078.
[14] E.H. Bae, J.S. Kim, B.W. Choi, K.K. Lee, Decoupled parameter estimation of multiple distributed sources for uniform linear array with low complexity, Electron. Lett. 44 (10) (May 2008) 649–650.
[15] M. Souden, S. Affes, J. Benesty, A two-stage approach to estimate the angles of arrival and the angular spreads of locally scattered sources, IEEE Trans. Signal Process. 56 (5) (May 2008) 1968–1983.
[16] J.A. Chaaya, J. Picheral, S. Marcos, Localization of spatially distributed near-field sources with unknown angular spread shape, Signal Process. 106 (Jan. 2015) 259–265.
[17] S.M. Wenmeng Xiong, José Picheral, Robustness of the coherently distributed MUSIC algorithm to the imperfect knowledge of the spatial distribution of the sources, Signal Image Video Process. 11 (4) (May 2017) 721–728.
[18] M.S. Xiong Wenmeng, Picheral José, Performance analysis of distributed source parameter estimator (DSPE) in the presence of modeling errors due to the spatial distributions of sources, Signal Process. 143 (Feb. 2018) 146–151.
[19] T. Trump, B. Ottersten, Estimation of nominal direction of arrival and angular spread using an array of sensors, Signal Process. 50 (1) (Apr. 1996) 57–69.
[20] O. Besson, F. Vincent, P. Stoica, A.B. Gershman, Approximate maximum likelihood estimators for array processing in multiplicative noise environments, IEEE Trans. Signal Process. 48 (9) (Sep. 2000) 2506–2518.
[21] B.T. Sieskul, An asymptotic maximum likelihood for joint estimation of nominal angles and angular spreads of multiple spatially distributed sources, IEEE Trans. Veh. Technol. 59 (3) (Mar. 2010) 1534–1538.
[22] M. Ghogho, O. Besson, A. Swami, Estimation of directions of arrival of multiple scattered sources, IEEE Trans. Signal Process. 49 (11) (Nov. 2001) 2467–2480.
[23] Y. Meng, P. Stoica, K. Wong, Estimation of the directions of arrival of spatially dispersed signals in array processing, IEE Proc. Radar Sonar Navig. 143 (1) (Feb. 1996) 1–9.
[24] M. Bengtsson, Antenna Array Signal Processing for High Rank Models, Ph.D. Dissertation, Royal Inst. Technol., Stockholm, Sweden, 1999.
[25] M. Bengtsson, B. Ottersten, A generalization of weighted subspace fitting to full-rank models, IEEE Trans. Signal Process. 49 (5) (May 2001) 1002–1012.
[26] A. Zoubir, Y. Wang, P. Chargé, Efficient subspace-based estimator for localization of multiple incoherently distributed sources, IEEE Trans. Signal Process. 56 (2) (Feb. 2008) 532–542.
[27] A. Hassanien, S. Shahbazpanahi, A.B. Gershman, A generalized Capon estimator for localization of multiple spread sources, IEEE Trans. Signal Process. 52 (1) (Jan. 2004) 280–283.
[28] J. Capon, High-resolution frequency-wavenumber spectrum analysis, Proc. IEEE 57 (8) (Aug. 1969) 1408–1418.
[29] A. Zoubir, Y. Wang, Robust generalised Capon algorithm for estimating the angular parameters of multiple incoherently distributed sources, IET Signal Process. 2 (2) (Jun. 2008) 163–168.
[30] B. Ottersten, P. Stoica, R. Roy, Covariance matching estimation techniques for array signal processing applications, Digit. Signal Process. 8 (3) (Jul. 1998) 185–210.
[31] O. Besson, P. Stoica, Decoupled estimation of DOA and angular spread for a spatially distributed source, IEEE Trans. Signal Process. 48 (7) (Jul. 2000) 1872–1882.
[32] A. Zoubir, Y. Wang, P. Chargé, A modified COMET-EXIP method for estimating a scattered source, Signal Process. 86 (4) (Apr. 2006) 733–743.
[33] S. Shahbazpanahi, S. Valaee, A.B. Gershman, A covariance fitting approach to parametric localization of multiple incoherently distributed sources, IEEE Trans. Signal Process. 52 (3) (Mar. 2004) 592–600.
[34] M. Bengtsson, B. Ottersten, Low-complexity estimators for distributed sources, IEEE Trans. Signal Process. 48 (8) (Aug. 2000) 2185–2194.
[35] F. Gao, A.B. Gershman, A generalized ESPRIT approach to direction-of-arrival estimation, IEEE Signal Process. Lett. 12 (3) (Mar. 2005) 254–257.
[36] R. Cao, F. Gao, X. Zhang, An angular parameter estimation method for incoherently distributed sources via generalized shift invariance, IEEE Trans. Signal Process. 64 (17) (Sep. 2016) 4493–4503.
[37] G. Xu, S.D. Silverstein, R.H. Roy, T. Kailath, Beamspace ESPRIT, IEEE Trans. Signal Process. 42 (2) (Feb. 1994) 349–356.
[38] R. Hamza, K. Buckley, Multiple cluster beamspace and resolution-enhanced ESPRIT, IEEE Trans. Antennas Propag. 42 (8) (Aug. 1994) 1041–1052.
[39] C.P. Mathews, Improved closed-form DOA/frequency estimation via ESPRIT using DFT and derivative DFT beamforming, in: Proc. IEEE International Conference on Acoustics, Speech and Signal Processing, ICASSP, Atlanta, GA, May 1996, vol. 5, 1996, pp. 2916–2919.
[40] G.M. Kautz, M.D. Zoltowski, Beamspace DOA estimation featuring multirate eigenvector processing, IEEE Trans. Signal Process. 44 (7) (Jul. 1996) 1765–1778.

Zhi Zheng received the M.S. and Ph.D. degrees in electronic engineering and information and communication engineering from the University of Electronic Science and Technology of China (UESTC), Chengdu, China, in 2007 and 2011, respectively. From 2014 to 2015, he was an Academic Visitor with the Department of Electrical and Electronic Engineering, Imperial College London. Since 2011, he has been with the School of Information and Communication Engineering, UESTC, where he is currently an Associate Professor. His area of interests include wireless communications, signal processing for communications, array signal processing, source localization, and array processing for radar and communications applications.

Jian Lu received the B.S. degree in communication engineering from the University of Electronic Science and Technology, Chengdu, China, in 2016, where he is currently pursuing the M.S. degree with the School of Information and Communication Engineering. His current research interests include array signal processing, especially direction-of-arrival estimation and source localization, wireless communications, and signal processing for communications.

Wen-Qin Wang received the B.S. degree in electrical engineering from Shandong University, China, in 2002, and the M.E. and Ph.D. degrees in information and communication engineering from the University of Electronic Science and Technology of China (UESTC), Chengdu, China, in 2005 and 2010, respectively. From 2005 to 2007, he was with the National Key Laboratory of Microwave Imaging Technology, Chinese Academy of Sciences, Beijing, China. From 2011 to 2012, he was a Visiting Scholar with the Stevens Institute of Technology, NJ, USA. From 2012 to 2013, he was a Hong Kong Scholar with the City University of Hong Kong, Hong Kong. From 2014 to 2016, he was a Marie Curie Fellow with the Imperial College London, U.K. Since 2007, he has been with the School of Information and Communication Engineering, UESTC, where he is currently a Professor. His research interests span the areas of array signal processing and circuit systems for radar and communications and microwave remote sensing. He was a recipient of the Marie Curie International Incoming Fellowship, the National Young Top-Notch Talent of the Ten-Thousand Talent Program Award, and the Hong Kong Scholar Fellowship. He is an editorial board member of four international journals.

Haifen Yang received her B.S.E. and M.S.E. degrees in Communication Engineering in 2000 and 2003, respectively, from the Department of Communication Engineering and Computer, Southwest Jiaotong University (SWJTU). In 2008, she received her Ph.D. degree University of Electronic and Science Technology of China (UESTC). From 2013 to 2014, she had been stayed in the University of California at Irvine (UCI) as a visiting scholar. She is currently an Associate Professor in the Department of Communication and Information Engineering at University of Electronic and Science Technology of China. Her general research interests include wireless communications and signal processing, with emphasis on massive MIMO and collaborative beamforming.

Shunsheng Zhang received the Ph.D. degree in signal and information processing from the Beijing Institute of Technology in 2007. In 2007, he joined the Research Institute of Electronic Science and Technology, University of Electronic Science and Technology of China. In 2009, he became an Associate Professor. From 2014 to 2015, he was a Visiting Scholar with the Department of Electrical and Computer Engineering, National University of Singapore. His major research interests include radar imaging (SAR/ISAR), array signal processing, and the applications of frequency diverse array.